Available online at www.sciencedirect.com
SCIENCE DIRECT®
Radiation Measurements 39 (2005) 515–519
Radiation Measurements
www.elsevier.com/locate/radmeas

Effects of the electric field on the electron drift velocity in a double-GEM detector in different gas mixtures

P.R.B. Marinho[a,*], G.P. Guedes[b], A.F. Barbosa[a], P.C.M.A. Farias[b,c]

[a]Centro Brasileiro de Pesquisas Físicas—CBPF, Rua Dr. Xavier Sigaud, 150, CEP 22290-180, Rio de Janeiro-RJ, Brazil
[b]Universidade Estadual de Feira de Santana—UEFS, BR 116 Km 3, CEP 44031-460 Feira de Santana-BA, Brazil
[c]Laboratório de Instrumentação Nuclear, COPPE-UFRJ P.O. Box 68509, CEP 21945-970, Rio de Janeiro-RJ, Brazil

Received 24 May 2004; received in revised form 13 August 2004; accepted 31 August 2004

Abstract

A study of the electronic drift velocity in a double-GEM detector is presented. We compare measurements and simulations done to investigate the effects of the induction parameters—electric field and gap—for different gas mixtures Ar/CH_4(90/10), Ar/C_2H_6(75/25), Ar/Xe/CO_2(64/16/20) and Ar/Kr/CO_2(76/19/5) at atmospheric pressure using 5.9 keV X-rays. We used 2, 4 and 6 mm deep induction gaps and induction fields varying up to 6 kV/cm.

Keywords: Gas electron multiplier; Gas mixtures; Gas gain; X-ray detection; Gaseous detector

1. Introduction

The gas electron multiplier (GEM) was introduced in 1997 by Sauli (1997). It consists of a 50 μm insulator foil, metal-clad on both sides, perforated with a high density of small holes (Bouianov et al., 2001; Benlloch et al., 1998). When a suitable voltage is applied on the GEM electrodes, a very strong electric field (above 40 kV/cm) arises within the holes, where the gas amplification process takes place (Bachmann et al., 2002).

Higher gains can be achieved using multiple GEMs assembled in cascade (Bachmann et al., 1999, 2002; Bellazzini et al., 1998). In this case, the electric fields between GEMs must be optimized to provide the maximum charge transfer and to reduce losses of electrons to the GEM electrodes (Bachmann et al., 1999; Richter et al., 2002). Moreover, as the induction field affects the electronic drift time, it modifies the shape of the anode signal (rise time and pulse width) (Guedes et al., 2003). The rise time and pulse width are important timing features of the anode signal needed to optimize the readout electronic as in the delay line technique used for 2D position sensitive detectors (Guedes et al., 2003).

This work reports on measurements of drift velocities through the analysis of the pulse width induced on the anode of a double-GEM detector in the gas mixtures Ar/CH_4(90/10), Ar/C_2H_6(75/25), Ar/Xe/CO_2(64/16/20) and Ar/Kr/CO_2(76/19/5) at atmospheric pressure, showing the dependence of the electron drift velocity on the induction electric field. We also compare the results to simulations done with the Magboltz program (Magboltz, 2002).

2. Apparatus and measurement procedures

The schematic setup of the double-GEM detector is shown in Fig. 1. The GEM size is $30 \times 30\ mm^2$, one of the standard types produced at CERN; the hole shape is double conical

* Corresponding author. Tel.: +55 21 21417371; fax: +55 21 21417400 .
E-mail address: renato@cbpf.br (P.R.B. Marinho).

1350-4487/$ - see front matter © 2004 Elsevier Ltd. All rights reserved.
doi:10.1016/j.radmeas.2004.08.004

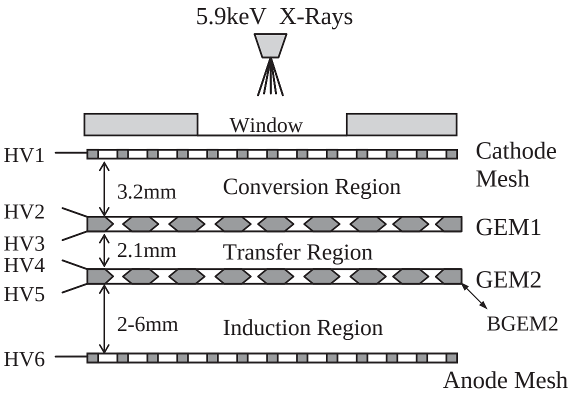

Fig. 1. Schematic view of the double-GEM detector.

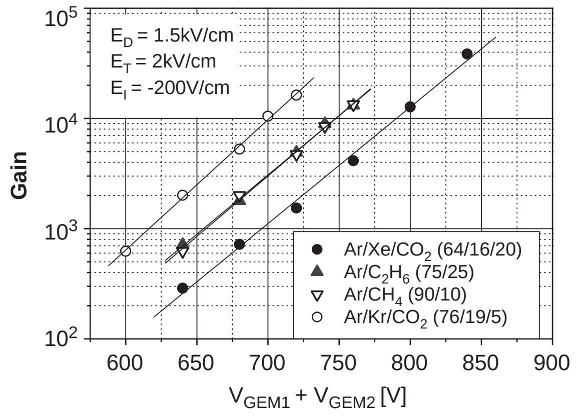

Fig. 2. Charge gain as a function of the applied voltage at the GEMs.

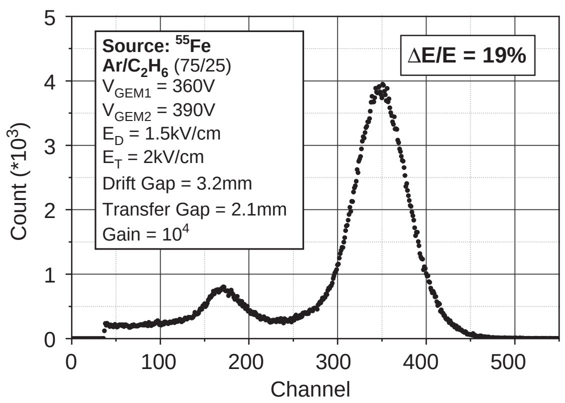

Fig. 3. Energy spectrum of ^{55}Fe source in gas mixing Ar/C_2H_6(75/25).

with an inner diameter of about 50 µm and 80 µm at the metal surface. The hole pitch is 140 µm arranged in a hexagonal pattern; the overall thickness of the GEM foil is about 60 µm : 50 µm thick Kapton with 5 µm copper on each side. For both the anode and drift cathode we used a metal mesh with 81% transparency. The anode was placed at three different distances (2, 4 and 6 mm) from the last GEM. The drift and transfer gaps were kept at 3.2 and 2.1 mm, respectively. The detector window is a 50 µm thick Kapton foil.

Each electrode was powered independently and the anode-induced signals were read through a decoupling circuit with a current amplifier of 8 ns time constant. The BGEM2 signal was used to characterize the detector gain and energy resolution by using a charge amplifier (Ortec 142H, sensitivity $=700$ mV/pC). Electrode polarization was such that the detector operated with a gain of about 10^4 in flow mode with Ar/CH_4(90/10), Ar/C_2H_6(75/25), $Ar/Xe/CO_2$(64/16/20) and $Ar/Kr/CO_2$(76/19/5) gas mixtures at atmospheric pressure. We used a 5.9 keV ^{55}Fe as the photon source.

The gain for each gas mixture was obtained recording the charge on the bottom electrode of the second GEM (BGEM2) with a weak reversed induction field $(-200\,V/cm)$ insuring full collection of the charges from the multiplication process on the BGEM2 electrode. The drift and transfer field were kept constant at 1.5 and 2 kV/cm, respectively. Fig. 2 shows the gain curves for the different gas mixtures. The energy resolution $(\Delta E/E)$ of the double-GEM detector, with ΔE measured as the FWHM of the main peak of the ^{55}Fe photon source, ranges from 19% to 20% for all gas mixtures, at a gain of 10^4. Fig. 3 shows the energy spectrum for Ar/C_2H_6(75/25).

2.1. Drift velocity

The knowledge of the drift velocity of electrons in gases is important to improve the performance of gaseous detectors. In general, drift chambers are used to measure the drift velocity of the electrons in gas mixtures (Sauli, 1977; Peisert and Sauli, 1984). However, different setups may be used to estimate the electronic drift velocity as Micromegas (Colas et al., 2002) and GEM (Guedes et al., 2003) detectors.

The motion of free electrons in gases may be described by the classical kinetic theory of gases (Peisert and Sauli, 1984; Huxley and Crompton, 1974). In this model, the thermal electrons under the action of an electric field acquire a motion in the direction of the field with drift velocity $v_{drift} = \mu E/p$, where μ is the electron mobility, E is the electrical field strength and p is the gas pressure (the ratio E/p is called the reduced field).

When electrons move through the induction region toward the anode, they induce a charge distribution on that electrode. Since the electric field is constant in this region, the induced current signal is a box-shaped pulse whose width is the drift time in this region. Examples of these signals recorded for two induction fields are shown in Fig. 4, where one can see

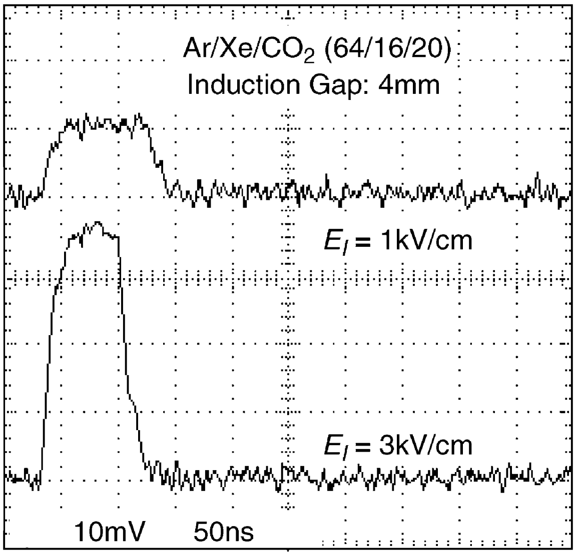

Fig. 4. Pulses recorded with current preamplifier on anode mesh in Ar/Xe/CO_2(64/16/20) for 4 mm gap for 1 and 3 kV/cm induction fields. The gain was kept constant (10^4).

the effect of the induction field on both the pulse width and the pulse height. One would expect the integral of the pulses to be the same in both cases. However, the induction field increases the gain due to the deformation of the electric field of the last GEM, which extends the amplification region toward the induction region (Guedes et al., 2003).

The drift time is proportional to the applied electric field. Therefore, it is possible to estimate v_{drift} by dividing the induction gap (d) by the pulse duration (t_w). The latter is taken as the interval from the rising edge to the falling edge, taken at the instants where the pulse reaches 50% of the maximum amplitude. The d error is related to the accuracy of the caliper used to measure it, and the t_w error is estimated in each signal record with the scope. Since the pulse shape in its rising and falling regions look like an S-curve, we may use a sigmoidal function to fit it. By differentiation of the S-curve, one obtains a Gaussian-shapes curve, whose width corresponds to the uncertainty associated with the time measurement. The t_w error is then taken as the sum of the standard deviations given by Gaussian fits to the differentiated S-curve in the rising and falling regions of the pulse. Finally, we can estimate the v_{drift} error by using the *error propagation formula* (Knoll, 1989). The error bars are shown in Fig. 5.

2.2. Simulations

In order to check the experimental results, we used the Magboltz program to simulate the electron drift velocity for the current set of gas mixtures. Magboltz computes the gas transport parameters in a wide range of electric and magnetic fields by solving the Boltzmann transport equation. For the drift velocity, the program computes the average value of the velocity distribution function. For every gas mixture we have entered the parameters according to the actual measurements: 1 atm pressure, 300 K temperature and an electric field ranging from 10 up to 6000 V/cm with no magnetic field.

3. Results and discussion

The electron drift velocities measured and simulated for different gas mixtures as a function of the induction field are shown in Fig. 5, where we observe a good agreement for fields larger than 2 kV/cm. At electric fields < 2 kV/cm, the width of the box-shaped pulse is difficult to record due to the poor signal-to-noise ratio.

All gas mixtures show roughly the some asymptotic behavior for their electronic velocities: the drift velocity reaches a plateau for sufficiently high induction electric field. The velocity saturates at about 2.7 cm/μs for Ar/CH_4(90/10), 4 cm/μs for Ar/C_2H_6(75/25), 6 cm/μs for Ar/Xe/CO_2(64/16/20) and 4 cm/μs for Ar/Kr/CO_2(76/19/5). Ar/CH_4(90/10) and Ar/C_2H_6(75/25) are well-known gas mixtures and their obtained asymptotic values agree with results in the literature (Peisert and Sauli, 1984; Becker et al., 1999; Colas et al., 2002). The experimental results obtained for Ar/Xe/CO_2(64/16/20) and Ar/Kr/CO_2(76/19/5) were not found in the literature and they agree with our simulations.

At low electric fields (< 1 kV/cm) we can see a similar behavior for Ar/CH_4(90/10), Ar/C_2H_6(75/25) and Ar/Kr/CO_2(76/19/5) gas mixtures: the electronic drift velocity increases abruptly and drops at somewhat higher fields. This occurs due to the Ramsauer effect (Schiff, 1955), where the scattering cross-section of electrons by gas is reduced considerably at low field (a few eV/cm). Therefore the electron mobility rises sharply at low fields and the drift velocity increases as well. At somewhat higher electric fields, the Ramsauer effect is minimized and the cross-section increases, consequently decreasing the electronic drift velocity.

For Ar/Xe/CO_2(64/16/20) gas mixture, we observe that the electronic drift velocity increases smoothly up to $\approx$ 2 kV/cm. This is expected because xenon is a 'slow' gas relative to argon (Becker et al., 1999). Besides, CO_2 is a cool quencher, i.e., it has a large inelastic cross-section for electron collisions, leaving the drifting electrons still thermal even for a large electric field (Peisert and Sauli, 1984).

4. Conclusion

We measured and simulated the drift velocity of electrons in Ar/CH_4(90/10), Ar/C_2H_6(75/25), Ar/Xe/CO_2(64/16/20) and Ar/Kr/CO_2(76/19/5) gas mixtures for a double-GEM

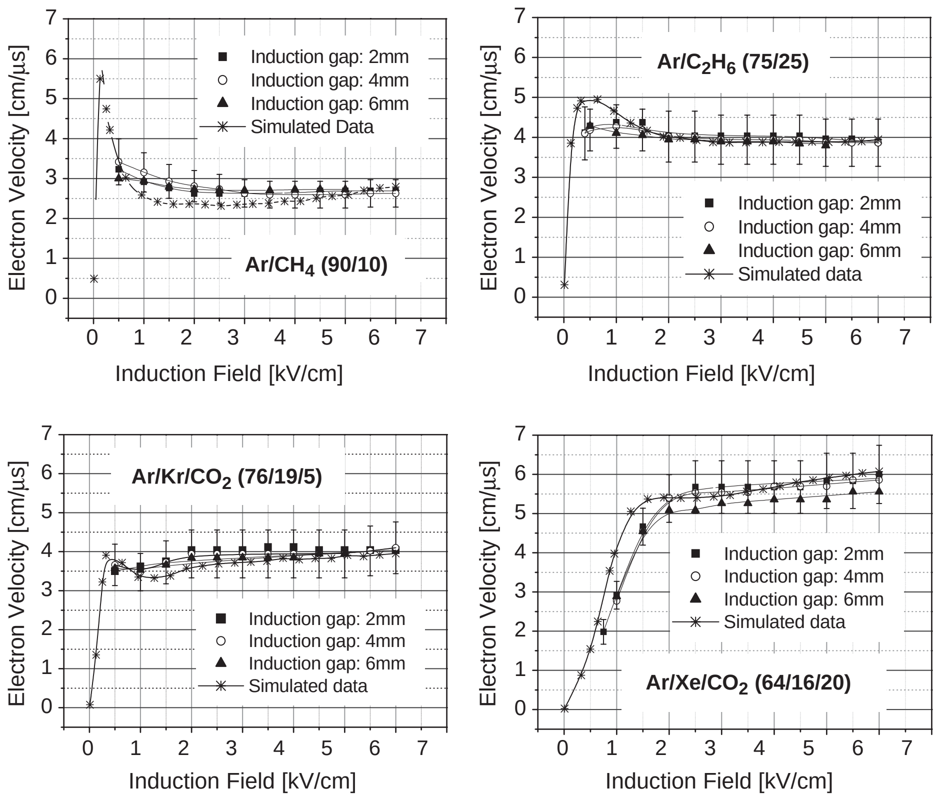

Fig. 5. Comparison between the drift velocity of electrons and drift velocity simulated in different gas mixtures versus induction field. The drift and transfer field were kept constant at 1.5 and 2 kV/cm, respectively. The lines are drawn to guide the eye.

setup with 2, 4 and 6 mm induction gaps. A good agreement between measured and simulated data is observed, especially for induction fields larger than 2 kV/cm. We have also found electronic drift velocity independence with respect to used gap.

This kind of result is important to optimize the detector parameters for systems used for 2D position readout. A good choice of the gas mixtures guarantees an approximately constant drift velocity for a wide range of the electric field, which is important for obtaining good position resolution and stable operation. Besides, we observed the effects of the induction fields and the gap on the anode signal shape. Based on these features, we can select the best anode signal (one with faster rise time and narrower width), optimizing the transmission through the readout system.

Finally, these results show that one may use the simple parallel-plate geometry of GEM setup to measure drift velocities through the analysis of the anode pulse shape.

Acknowledgements

The authors are grateful to CNPq (Brazilian national research funding agency) for the financial support. Our laboratory is a unit of CBPF, which is financially supported by the Brazilian Ministry of Science and Technology, and has received grants from FAPERJ and PADCT in its implementation stage.

References

Bachmann, S., et al., 2002. Nucl. Instrum. Methods A 479, 294.
Bachmann, S., et al., 1999. Nucl. Instrum. Methods A 438, 376.
Becker, U., et al., 1999. Nucl. Instrum. Methods A 421, 54.
Bellazzini, R., et al., 1998. Nucl. Instrum. Methods A 419, 429.
Benlloch, J., et al., 1998. Nucl. Instrum. Methods A 419, 410.
Bouianov, O., Bouianov, M., Orava, R., Tikhonov, V., 2001. Nucl. Instrum. Methods A 458, 698.
Colas, P., et al., 2002. Nucl. Instrum. Methods A 478, 215.
Guedes, G.P., Breskin, A., Chechik, R., Morman, D., 2003. Nucl. Instrum. Methods A 497, 305.
Guedes, G.P., Breskin, A., Chechik, R., Vartsky, D., Bar, D., Barbosa, A.F., Marinho, P.R.B., 2003. Nucl. Instrum. Methods A 513, 473.
Huxley, L.G.H., Crompton, R.W., 1974. The Diffusion and Drift of Electrons in Gases, Wiley, New York.
Knoll, G.F., 1989. Radiation Detection and Measurement, Wiley, New York. p. 88.

Magboltz, CERN Transport of Electron in Gas Mixtures Computation Program written by S. F. Biagi, Version 3, 2002.

Peisert, A., Sauli, F., 1984. Drift and Diffusion of electrons in gases: a compilation. CERN 84-08.

Richter, C., Breskin, A., Chechik, R., Garty, G., Sharma, A., 2002. Nucl. Instrum. Methods A 478, 538.

Sauli, F., 1977. Principles of operation of multiwire proportional and drift chambers. CERN 77-09.

Sauli, F., 1997. Nucl. Instrum. Methods A 386, 531.

Schiff, L.I., 1955. Quantum Mechanics, McGraw-Hill, New York. p. 108.